World Journal of Gastroenterology

Submit a Manuscript: https://www.f6publishing.com

World J Gastroenterol 2024 May 28; 30(20): 2689-2708

DOI: 10.3748/wjg.v30.i20.2689

ISSN 1007-9327 (print) ISSN 2219-2840 (online)

ORIGINAL ARTICLE

Basic Study

Kinesin 26B modulates M2 polarization of macrophage by activating cancer-associated fibroblasts to aggravate gastric cancer occurrence and metastasis

Lian-Meng Huang, Ming-Jin Zhang

Specialty type: Gastroenterology and hepatology

Provenance and peer review: Unsolicited article; Externally peer reviewed.

Peer-review model: Single blind

Peer-review report's classification

Scientific Quality: Grade B, Grade B, Grade B, Grade C, Grade C

Novelty: Grade B, Grade B, Grade B, Grade B, Grade B

Creativity or Innovation: Grade B, Grade B, Grade B, Grade B, Grade B

Scientific Significance: Grade B, Grade B, Grade B, Grade B, Grade B

P-Reviewer: Elkady N, Egypt; Muzes G, Hungary; Nakaji K, Japan; Rodrigo L, Spain

Received: December 15, 2023

Revised: February 28, 2024

Accepted: April 19, 2024

Published online: May 28, 2024

Lian-Meng Huang, Ming-Jin Zhang, Department of General Surgery, The 901st Hospital of PLA, Hefei 230031, Anhui Province, China

Corresponding author: Ming-Jin Zhang, MD, Professor, Department of General Surgery, The 901st Hospital of PLA, No. 424 Changjiang West Road, Shushan District, Hefei 230031, Anhui Province, China. zhangmingjin2001@163.com

Abstract

BACKGROUND

The regulatory effects of *KIF26B* on gastric cancer (GC) have been confirmed, but the specific mechanism still needs further exploration. Pan-cancer analysis shows that the *KIF26B* expression is highly related to immune infiltration of cancer-associated fibroblasts (CAFs), and CAFs promote macrophage M2 polarization and affect cancers' progression.

AIM

To investigate the regulatory functions of *KIF26B* on immune and metastasis of GC.

METHODS

We analyzed genes' mRNA levels by quantitative real-time polymerase chain reaction. Expression levels of target proteins were detected by immunohisto-chemistry, ELISA, and Western blotting. We injected AGS cells into nude mice for the establishment of a xenograft tumor model and observed the occurrence and metastasis of GC. The degree of inflammatory infiltration in pulmonary nodes was observed through hematoxylin-eosin staining. Transwell and wound healing assays were performed for the evaluation of cell invasion and migration ability. Tube formation assay was used for detecting angiogenesis. M2-polarized macrophages were estimated by immunofluorescence and flow cytometry.

RESULTS

KIF26B was significantly overexpressed in cells and tissues of GC, and the higher expression of *KIF26B* was related to GC metastasis and prognosis. According to *in vivo* experiments, *KIF26B* promoted tumor formation and metastasis of GC. *KIF26B* expression was positively associated with CAFs' degree of infiltration. Moreover, CAFs could regulate M2-type polarization of macrophages, affecting

GC cells' migration, angiogenesis, invasion, and epithelial-mesenchymal transition process.

CONCLUSION

KIF26B regulated M2 polarization of macrophage through activating CAFs, regulating the occurrence and metastasis of GC.

Key Words: *KIF26B*; Gastric cancer; M2 polarization macrophage; Cancer-associated fibroblasts; Immunity; Metastasis

©The Author(s) 2024. Published by Baishideng Publishing Group Inc. All rights reserved.

Core Tip: *KIF26B* could promote cancer-associated fibroblast activation, mediating macrophage M2 polarization and affecting the occurrence, lung metastasis, and abdominal metastasis of gastric cancer (GC). This study provides useful insights for exploring new mechanisms of GC and suppressing its progression.

Citation: Huang LM, Zhang MJ. Kinesin 26B modulates M2 polarization of macrophage by activating cancer-associated fibroblasts to aggravate gastric cancer occurrence and metastasis. *World J Gastroenterol* 2024; 30(20): 2689-2708
URL: https://www.wjgnet.com/1007-9327/full/v30/i20/2689.htm
DOI: https://dx.doi.org/10.3748/wjg.v30.i20.2689

INTRODUCTION

Kinesin superfamily proteins (KIFs), known as molecular motor proteins, were dependent on microtubule or ATP and were used to transport membrane organelle[1-3]. KIFs have been identified as potential molecular targets in cancer treatment[4-6]. This study was based on the KIFs, and bioinformatics analysis was conducted to screen out the most likely potential gene (*KIF26B*) involved in gastric cancer (GC) progression and prognosis.

KIFs participate in the regulation of multiple cancers. Silencing of *KIF15* can reduce cell proliferation and enhance cell apoptosis to retard the progression of osteosarcoma[7]. *KIF11* aggravates the progression of breast cancer and results in poor prognosis[8]. *KIF20B* strengthens tumorigenesis in tongue cancer[9]. Suppression of *KIF15* weakens cell proliferation to inhibit the progression of triple-negative breast cancer[10]. A study has confirmed the role of the KIFs in GC, such as *KIF15* promotes GC progression by promoting proliferation and inhibiting apoptosis[11], and *KIF2A* downregulation inhibits GC cell invasion by inhibiting MT1-MMP[12]. Little research has focused on the regulation of GC progression by *KIF26B*. One study from 2017 suggests that *KIF26B* promotes GC cell proliferation and metastasis through VEGF pathway activation[13].

In recent years, many literatures have verified that tumor microenvironment (TME) promotes tumor occurrence, progression, and metastasis[14-16]. One of the main functions of TME is to stimulate the immunosuppressive environment around tumors through various mechanisms[17,18]. Cancer-associated fibroblasts (CAFs) are the key cells in TME[18,19]. According to pan-cancer analysis, *KIF26B* expression is highly associated with CAF immune infiltration[20].

Macrophages interact with tumor cells in the TME and cause tumor progression[21]. M1 polarization of macrophage is characterized by increased pro-inflammatory activity, enhanced antigen presentation, and tumor growth inhibition[22,23]. Macrophages' M2 polarization contributes to malignant angiogenesis, tumor cell proliferation, and growth[24,25]. Cancer cells regulate macrophages to aggravate tumor metastasis[26]. A study has illustrated the relationship axis between CAFs/macrophages/cancer cells, indicating that CAFs can promote macrophage M2 polarization by secreting CXCR12, thereby affecting cancer cell behavior and worsening cancer prognosis[27].

We hypothesized that *KIF26B* might regulate immune suppression and metastasis of GC through influencing CAF immune infiltration in this study.

MATERIALS AND METHODS

Clinical samples

We obtained tumor and adjacent normal tissues in pairs (n = 50) from GC patients from July 2019 to March 2023. This study was approved by the Medical Ethics Committee of The 901st Hospital of PLA (No. 202311006). The written consent from each participant has been acquired.

Survival prognosis analysis

To verify GC patients in the high-*KIF26B* or low-*KIF26B* expression subgroups, the Kaplan-Meier analysis with the "survminer" R package was performed. The log-rank test was utilized to determine the significance of differences.

Quantitative real-time polymerase chain reaction

We extracted total RNAs from frozen tissues by the Trizol reagent (Invitrogen, Carlsbad, CA, United States). Complementary DNA from RNAs was synthesized through the reverse transcription kit (Invitrogen, Carlsbad, CA, United States). Quantitative real-time polymerase chain reaction (qRT-PCR) was made through a SYBR® Green qRT-PCR Kit (Promega, Madison, WI, United States). We calculated relative mRNA expression levels by means of the $2^{-\Delta\Delta ct}$ method (GAPDH as the internal reference).

Primer sequences: *KIF26B*, forward: 5′-CCACCUCUUU GAGAAGGATT-3′, reverse: 5′-UUCCUUCUCAAAGAGGUGGTT-3′; *α-SMA*, forward: 5′-CGCCCTCGCCACCAGATCTG-3′, reverse: 5′-TAGCCTTCATAGATG GGGAC-3′; *ACTA2*, forward: 5′-GAGGGAAGGTCCTAACAGCC-3′, reverse: 5′-GCTTCACAGGATTCCCGTCT-3′; *CXCL12*, forward, 5′-CCGCGCTCTGCCT CAGCGACGGGAAG-3′, reverse, 5′-CTTGTTTAAAGCTTTCTCCAGGTACT-3′; *FAP*, forward: 5′-TGGGTGTCCAGT-GAACGAGTATG-3′, reverse: 5′-TGTATTT CTTGGTCTGTGCGGC-3′; *ITGB1*, forward: 5′-CCTCTCAGCCTCCAGCGTTG-3′, reverse: 5′-TGCTCTTGCTCACTCACACTCC-3′; *PDPN*, forward: 5′-CGAAGATG ATGTGGTGACTC-3′, reverse: 5′-CGATGCGAATGCCTGTTAC-3′; *THY1*, forward: 5′-GAAGGTCCTCTACTT ATCCGCC-3′, reverse: 5′-TGATGCCCTCACA CTTGACCAG-3′; *GAPDH*, forward: 5′-GGTGAAGGTCGGAGTCAACG-3′, reverse: 5′-CAAAGTTGTCATGGATGHACC-3′.

Immunohistochemistry staining

We collected paraffin sections of GC tumor tissues and normal adjacent tissues (n = 3) from GC patients as well as tumor tissues from mice. Tumor tissues were fixed, embedded (paraffin), and sliced into sections (4 μm thick). We deparaffinized paraffin sections and then rehydrated them, and restoring the antigen was carried out by means of citrate buffer at a high temperature and pH of 6.0. We incubated these sections mixed with primary antibody anti-*KIF26B* (ab121952, 1/200, Abcam), anti-Ki67 (ab15580, 0.1 μg/mL, Abcam), anti-α-SMA (ab5694, 1/200, Abcam) and anti-CD163 (ab182422, 1/500, Abcam) at 4 °C overnight. These sections were washed by incubation with secondary antibodies Goat F (ab')2 Anti-Rabbit IgG F (ab')2 (HRP) (ab6112, 1: 500, Abcam) for 30 min. The sections were stained with hematoxylin and diaminobenzidine and observed under a microscope. The immunohistochemistry (IHC) images were analyzed through Image J software.

Cell transfection

We purchased HGC-27/AGS and GES-1 cells from the Cell Bank of the Chinese Academy of Sciences (Shanghai, China) and cultured them in RPMI-1640 medium with 10% foetal bovine serum (FBS) and 1% penicillin at 37 °C in an incubator with 5% CO_2.

The plasmids (RiboBio, Beijing, China), including sh-*KIF26B*, pcDNA-*KIF26B*, and negative controls (sh-NC, pcDNA-NC) were utilized. We transfected above mentioned plasmids into HGC-27 and AGS cells with Lipofectamine 3000 (Invitrogen, United States) and cultured them for 24 h. The transfection efficiency was detected utilizing western blotting.

Nude mice tumorigenesis assay

We bought mice (5-wk-old; BALB/c nude mice; males) from Vital River Laboratories (Beijing, China). All mice were maintained under controlled conditions (12 h light/dark, temperature: 22–24 °C, humidity: 40%–60%) and were offered free food and sterilized water. AGS cells (5×10^6) transfected with sh-*KIF26B*/sh-NC were injected into the mice's inguinal skin. After four weeks, we killed nude mice with an overdose of pentobarbital. All animal experiments were approved by the Animal Ethics Committee of Beijing Viewsolid Biotechnology Co. LTD (No. VS2126A00168). The authors read the ARRIVE Guidelines, and the manuscript was prepared and revised according to the ARRIVE Guidelines. After 28 d, mice were euthanized (the cervical dislocation method), and tumors were removed and weighed. The nodules of lung metastasis and intraperitoneal metastasis were counted. The experimental methods of mice were shown in Supplementary Figure 1.

Western blotting

We dissolved the HGC-27 cells with RIPA buffer (Beyotime, Shanghai, China), and the total protein was purified and quantified through bicinchoninic acid protein kits (ThermoFisher, United States). We detached proteins by 10% SDS-PAGE and moved them to PVDF membranes. After blocking with skimmed milk (5%), we incubated proteins with the primary antibodies anti-KIF26B (1:1000, FNab04559, FineTest, Wuhan, China), anti-E-cadherin (1:2000, ab40772, Abcam), anti-MMP-2 (1:5000, ab92536, Abcam), anti-N-cadherin (1:2000, ab76011, Abcam), anti-MMP-9 (1:5000, ab76003, Abcam) and anti-β-actin (1:2000, ab8227, Abcam) overnight at 4 °C. Proteins were incubated with the anti-rabbit secondary antibody (1:5,000; SA00001-2, SanYing, China) for one hour. We examined protein blots by the ECL chemiluminescent system. Image J was applied for the quantification of protein blots.

ELISA

We resuspended the HGC-27 cells (1×10^5) with 300 μL of complete medium, plated them in 96-well plates, and collected the supernatant after 3 d. ELISA was performed according to ELISA kits' instructions (Invitrogen, United States). We detected and recorded the absorbance value at 450 nm.

Transwell assay

In order to evaluate the ability of cell invasion, the transwell chamber was used. The supernatant (500 μL) collected from HGC-27 or CAFs was added into the upper chamber. Into the bottom chamber, we appended the serum-free medium

(about 200 µL). Then, the cell plate was cultured for 2 d at 37 °C with 5% CO_2. We removed the bottom chamber's cells with cotton swabs, and the upper chamber's cells were exposed to crystal violet (0.2%) to stain for 5 min. We used the inverted microscope for counting the number of invasion cells.

Flow cytometry

We cultured THP-1 monocytes in 6-well plates (10^6 cells/well) in RPMI medium together with 5% FBS and the supernatant of CAFs transfected with sh-*KIF26B*, pcDNA-*KIF26B*, and negative controls for 72 h. The macrophages were separated and incubated in a complete medium with 0.02% NaN3 for 30 min on ice. The incubation of macrophages with blocking antibodies anti-CD14/anti-CD206 and anti-F4/80/anti-CD206 (BD Biosciences Pharmingen, United States) was done for 20 min in Brilliant stain buffer on ice. We fixed the cells with 1% paraformaldehyde and performed the flow cytometric acquisition by BD LSR Fortessa (Flow cytometry, BD Biosciences Pharmingen, United States). The data analysis was made through FlowJoTM 10.8.1 software.

Immunofluorescence assay

We used an immunofluorescence assay for the detection of CD206 expression. CD206 is the marker of M2 macrophages. THP-1 cells were cultured to 70% confluence on the glass side. After washing twice with 1 × PBS, we fixed the cells with 4% paraformaldehyde for 1 h at 25 °C. We permeabilized cells with 0.2% Triton X-100 (X100, Sigma) in 1 × PBS at 37 °C for 15 min and closed by 10% normal goat serum at room temperature for 1 h. We incubated the cells with an anti-Mannose Receptor antibody (Abcam, ab64693, dilution 1 µg/mL) overnight at 4 °C. After PBS-washing, we incubated the cells with the goat anti-mouse IgG Alexa 488 conjugated fluorescence secondary antibody (R37120, dilution 1/1000) for 1 h at room temperature. We stained the cells with DAPI and observed them under a microscope.

Wound healing assay

We incubated AGS and HGC-27 cells (3×10^5 cells/well) in 6-well plates with a complete medium with extracellular matrix molecule (10 µg/mL) until the cell monolayer was formed. We used a pipette tip (200 µL) to scratch a straight line on the plate bottom. Next, we cultured AGS and HGC-27 cells with a medium (serum-free) for 1 d. We observed the wound-healing distance of both types of cells and gauged them by an inverted microscope (Carl Zeiss, Oberkochen, Germany).

Tube formation assays

HUVECs (2×10^4) were inoculated onto the 96-well plate coated with Matrigel, and the supernatant of CAFs was added. After culturing for 8 h, the tubular structure of HUVECs was observed under the inverted microscope.

Statistical analysis

Data were represented by the mean ± SD of three independent experiments. GraphPad Prism 7.0 (GraphPad Software, United States) was used for statistical analysis. Multiple group differences were analyzed using a one-way analysis of variance. Two group comparisons were performed using a Student's *t*-test. $P < 0.05$ indicates a statistical significance value.

RESULTS

Overexpression of KIF26B in GC and its poor prognosis

We examined kinesin superfamily expression levels in normal and tumor tissues and identified 18 DEGs (differentially expressed genes), of which 17 showed up-regulation, and 1 showed down-regulation (Figure 1A). We listed the DEGs of KIFs and quantified them, and found that the most significant difference in expression of *KIF26B* was observed in GC tissues (Supplementary Table 1). According to survival analysis, higher *KIF26B* expression resulted in poor prognosis (Figure 1B). We chose *KIF26B* as the follow-up study gene. We conducted a pan-cancer analysis on *KIF26B* and found that *KIF26B* was up-regulated in most cancers, with markedly significant differences in stomach adenocarcinoma (Figure 1C). qRT-PCR demonstrated that *KIF26B* expression was higher in GC tissues than in normal tissues (Figure 1D). IHC results presented high KIF26B (located in the cytoplasm) protein expression in GC tissues from patients (Figure 1E). Western blotting indicated that KIF26B protein expression in HGC-27/AGS cells was markedly higher compared with that in GES-1 cells (Figure 1F). A significant relation between high levels of *KIF26B* and infiltration depth, distant metastasis, lymph node metastasis, and tumor-node-metastasis (TNM) staging (T1 + T2 *vs* T3 + T4) was observed (Table 1).

KIF26B's effect on tumorigenesis, lung metastasis, and abdominal metastasis

We determined a xenograft tumor nude mouse model. We learned from the xenograft tumor experiment that knockdown of *KIF26B* could inhibit tumor growth of GC (Figure 2A-C). Immunohistochemical results demonstrated that *KIF26B* and Ki67 (located in the nucleus) expression levels were decreased after *KIF26B* suppression in tumor tissues from mice, indicating that there was an inhibition on the proliferative activity of GC cells after knocking down *KIF26B* (Figure 2D). The GC cells in the sh-*KIF26B* group decreased their metastasis to the pulmonary lymph node compared with the sh-NC group (Figure 2E and F). Knockdown of *KIF26B* inhibited the metastasis of GC cells to the peritoneum (Figure 2G and H). Knockdown of *KIF26B* could inhibit the occurrence of tumors, lung metastasis, and abdominal metastasis of GC *in vivo.*

A

Group
Status
Age
Stage
T
N
M
Grade
Gender

KIF5B
KIF1C
KIF3B
KIF1A
KIF6
KIF25
KIF4B
KIF2B
KIF5A
KIF17
KIF5C
KIF19
KIF12
KIF13B
KIF2A
KIF16B
KIF13A
KIF1B
KIF23
KIF20B
KIF20A
KIF4A
KIF18B
KIF22
KIF11
KIF2C
KIFC1
KIF26A
KIF27
KIF7
KIF3C
KIFC3
KIF21A
KIFC2
KIF26B
KIF14
KIF10
KIF15
KIF18A
KIF21B
KIF3A
KIF9
KIF24

10
8
6
4
2
0

Group
CON
STAD

Status
Alive
Dead
Not reported

Age
90
40

Stage
Stage I
Stage II
Stage III
Stage IV

T
T1
T2
T3
T4
TX

N
N0
N1
N2
N3
NX

M
M0
M1

Grade
G1
G2
G3

Gender
Female
Male

B

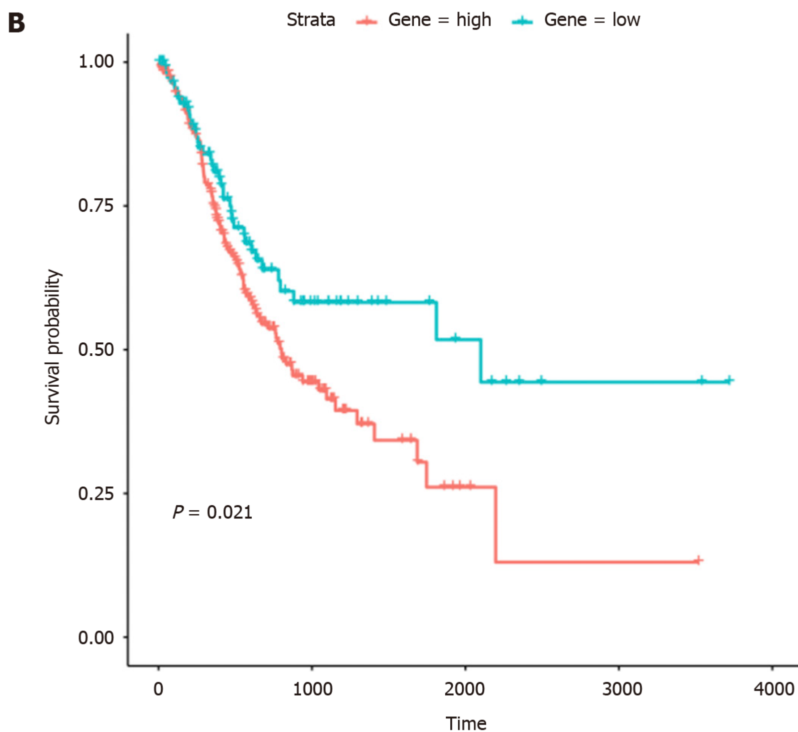

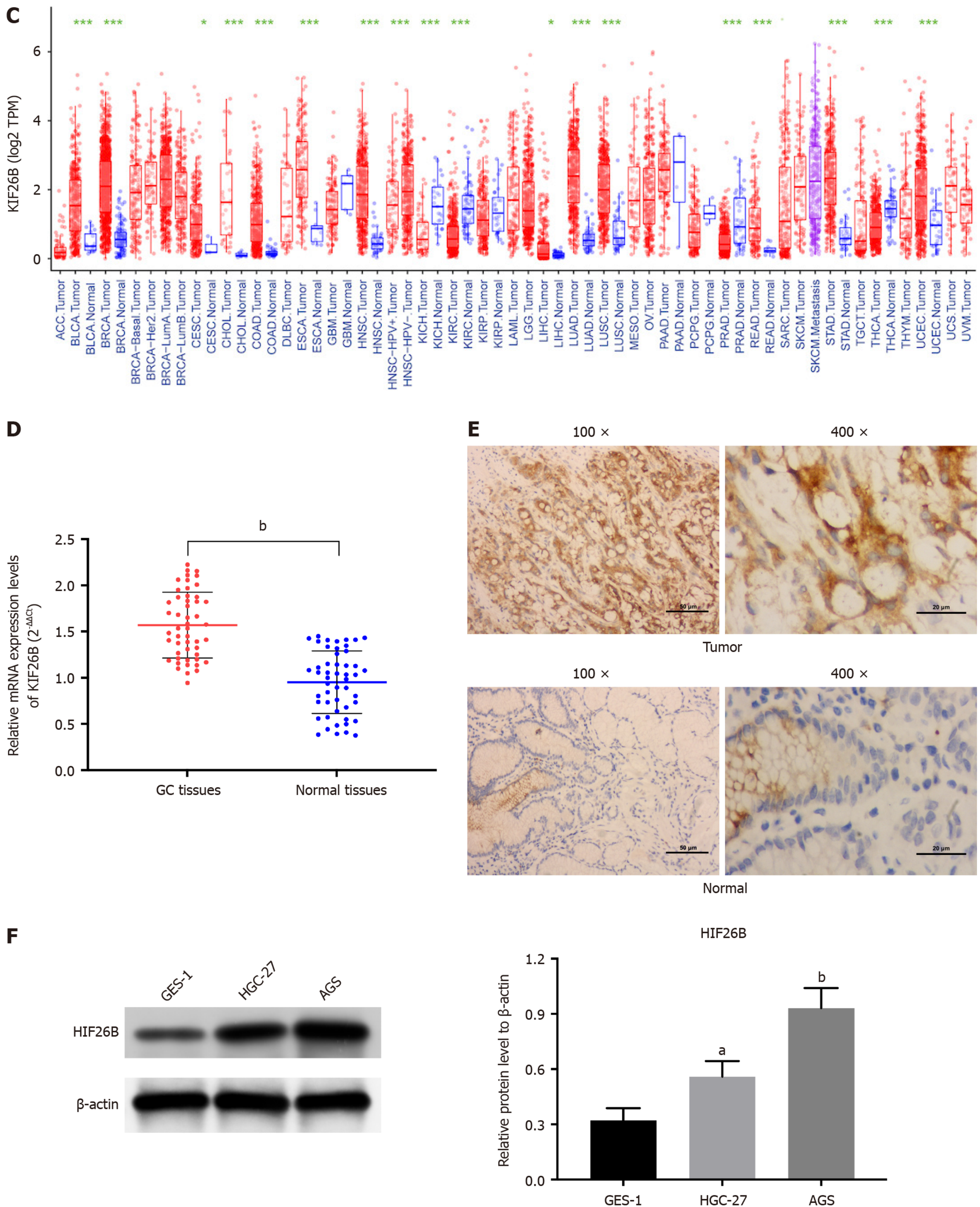

Figure 1 Overexpression of *KIF26B* in gastric cancer and its poor prognosis. A: The heat map shows the TCGA expression profile of all Kinesin superfamily proteins (normal and tumor tissues), with a total of 18 DEGs; B: The gene *KIF26B* with the most significant differential expression in gastric cancer (GC) was screened, and survival analysis was conducted; C: A pan-cancer analysis was conducted on *KIF26B* in various cancers; D: Using quantitative real-time polymerase chain reaction to detect the expression of *KIF26B* in GC tissue and adjacent tissues (n = 50); E: Immunohistochemical analysis of the expression of *KIF26B* in GC tissue and adjacent tissues (n = 3); F: The protein expression levels of KIF26B in GC cell lines (HGC-27/AGS) and normal gastric mucosal epithelial cell line (GES-1) were detected by western blotting (n = 3). [a]P < 0.05, [b]P < 0.01. GC: Gastric cancer.

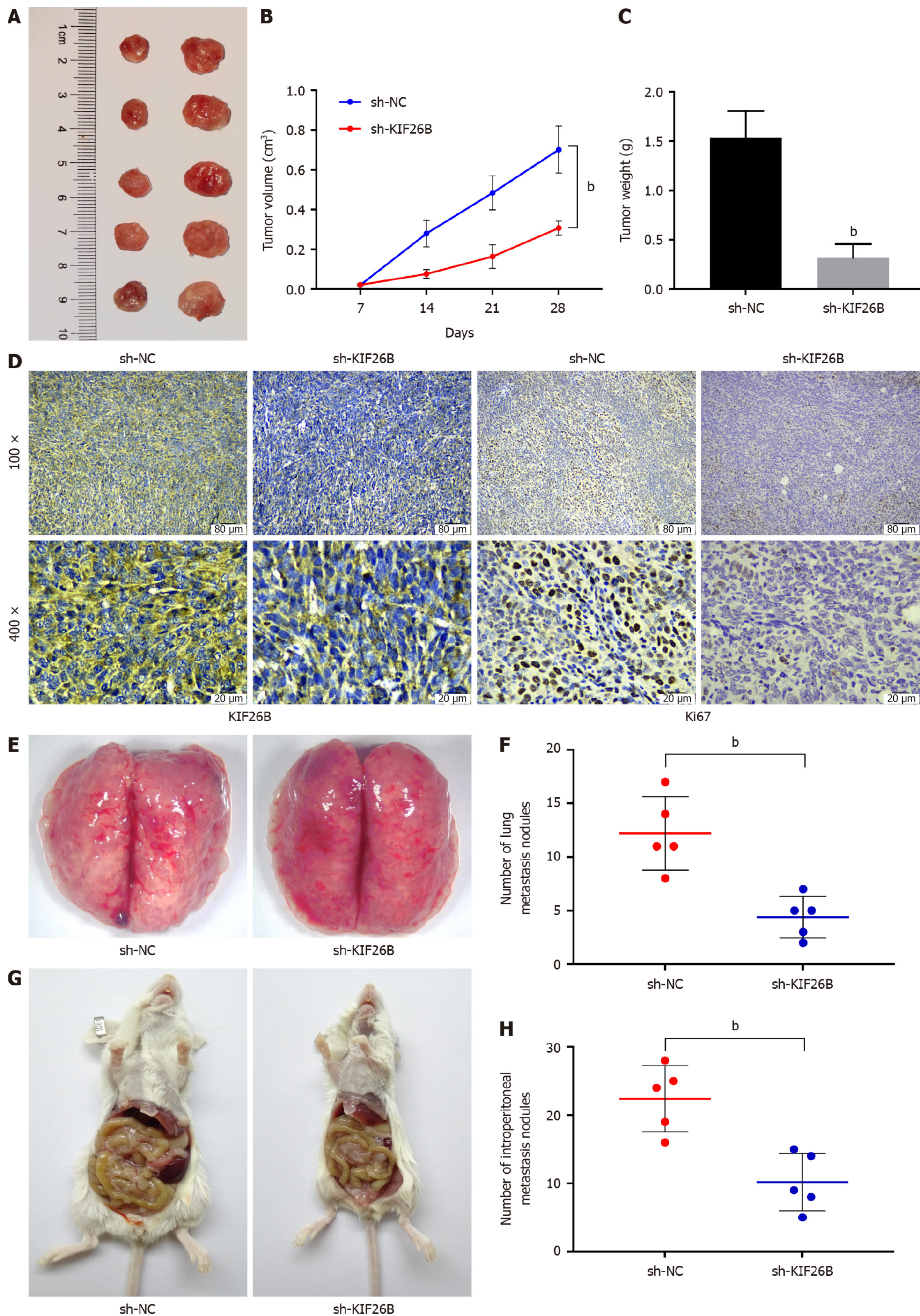

Figure 2 *KIF26B*'s effect on tumorigenesis, lung metastasis, and abdominal metastasis. A: Tumor images of xenograft tumors in nude mice; B: Volume changes of xenograft tumors in nude mice within 28 d; C: Weight of xenograft tumors in nude mice; D: Immunohistochemical analysis of KIF26B and Ki67 expression in tumor tissue; E: Image of tumor metastasis to lung lymph nodes to detect inflammatory infiltration in lung lymph nodes; F: Quantitative analysis of pulmonary nodules; G: Images of tumor metastasis to the peritoneum; H: Quantitative analysis of peritoneal nodules. $n = 5$. $^bP < 0.01$. sh-NC: sh-*KIF26B* negative controls.

Table 1 Association between clinical parameters of gastric cancer patients and KIF26B expression

Variable	Total	KIF26B expression (*n* = 50)		*P* value
		Low	High	
Age				0.5215
< 60 yr	18	9	9	
60 yr	32	19	13	
Sex				0.7412
Female	23	13	10	
Male	27	14	13	
Tumor size, cm				0.0336[a]
< 2	32	17	15	
2	18	4	14	
TNM stage				0.0016[b]
I/II	30	18	12	
III/IV	20	3	17	
Lymph node metastasis				0.0227[a]
Negative	25	15	10	
Positive	25	7	18	
Peritoneal metastasis				0.0009[c]
Negative	29	16	13	
Positive	21	2	19	

[a]$P < 0.05$.
[b]$P < 0.01$.
[c]$P < 0.0001$.
TNM stage: Tumor node metastasis stage.

High expression of KIF26B may affect the activation or infiltration of GC-related fibroblasts

KIF26B is highly correlated with the infiltration degree of CAFs, followed by endothelial cells (Figure 3A and B). We found a positive correlation between expression levels of *KIF26B* and *PD-1* (PDCD1) and *PD-L1* (CD274) (Figure 3C). To verify the correlation between *KIF26B* and the CAFs, we utilized the Timer 2.0 database. We confirmed that *KIF26B* was significantly correlated with CAFs biomarkers, such as *ACTA2*, *FAP*, *ITGB1*, *PDPN*, and *THY1* (Figure 3D). In the meanwhile, IHC experiments have found that both KIF26B and α-SMA (activation biomarker of CAFs) can be detected simultaneously in GC tissue from patients (Figure 3E). The results of qRT-PCR confirmed that *α-SMA*/*ACTA2* mRNA in metastatic GC tissues were markedly higher while comparing with non-metastatic GC tissues (Figure 3F). High expression of *KIF26B* may affect the activation and infiltration of CAFs, influencing the metastasis of GC.

KIF26B affects the activation of fibroblasts to form the CAF phenotype

We incubated primary human foreskin fibroblasts (HFF) with the supernatant of sh-*KIF26B* and sh-NC-transfected HGC-27 cells. The transfection's efficacy was confirmed by western blotting (Figure 4A). qRT-PCR and ELISA assays were used for detecting chemokines (*CXCL12*) in HFF cells, and *KIF26B* knockdown decreased *CXCL12* expression, indicating reducing the chemotaxis of HFF cells (Figure 4B and C). The transwell assay also demonstrated that suppression of *KIF26B* could decline HFF's invasive ability (Figure 4D). We detected the biomarkers of CAFs, including *α-SMA*, *FAP*, *ITGB1*, *PDPN*, and *THY1*, and inhibition of *KIF26B* decreased the expression levels of CAFs biomarkers (Figure 4E). It indicates that *KIF26B* can promote the activation of fibroblasts to form the CAF phenotype.

KIF26B enhances crosstalk between CAFs and macrophages, mediating M2 polarization of macrophages

A positive relation was found between *KIF26B* expression and the number of M2 macrophages (Figure 5A and B). Immunohistochemical results reported that *KIF26B* and CD163+ expressions were increased in GC tissues (high infiltration) from patients, indicating that *KIF26B* expression was positively related with the CD163+ expression (Biomarker of M2 macrophage) (Figure 5C). We transfected primary CAFs with sh-*KIF26B*, collected the supernatant and incubated THP-1 cells (induced by 100 ng/mL). Immunofluorescence assay detected CD206 (Surface biomarker of M2 macrophage) in THP-1 cells and indicated that the fluorescence intensity in the sh-*KIF26B* group was decreased markedly compared

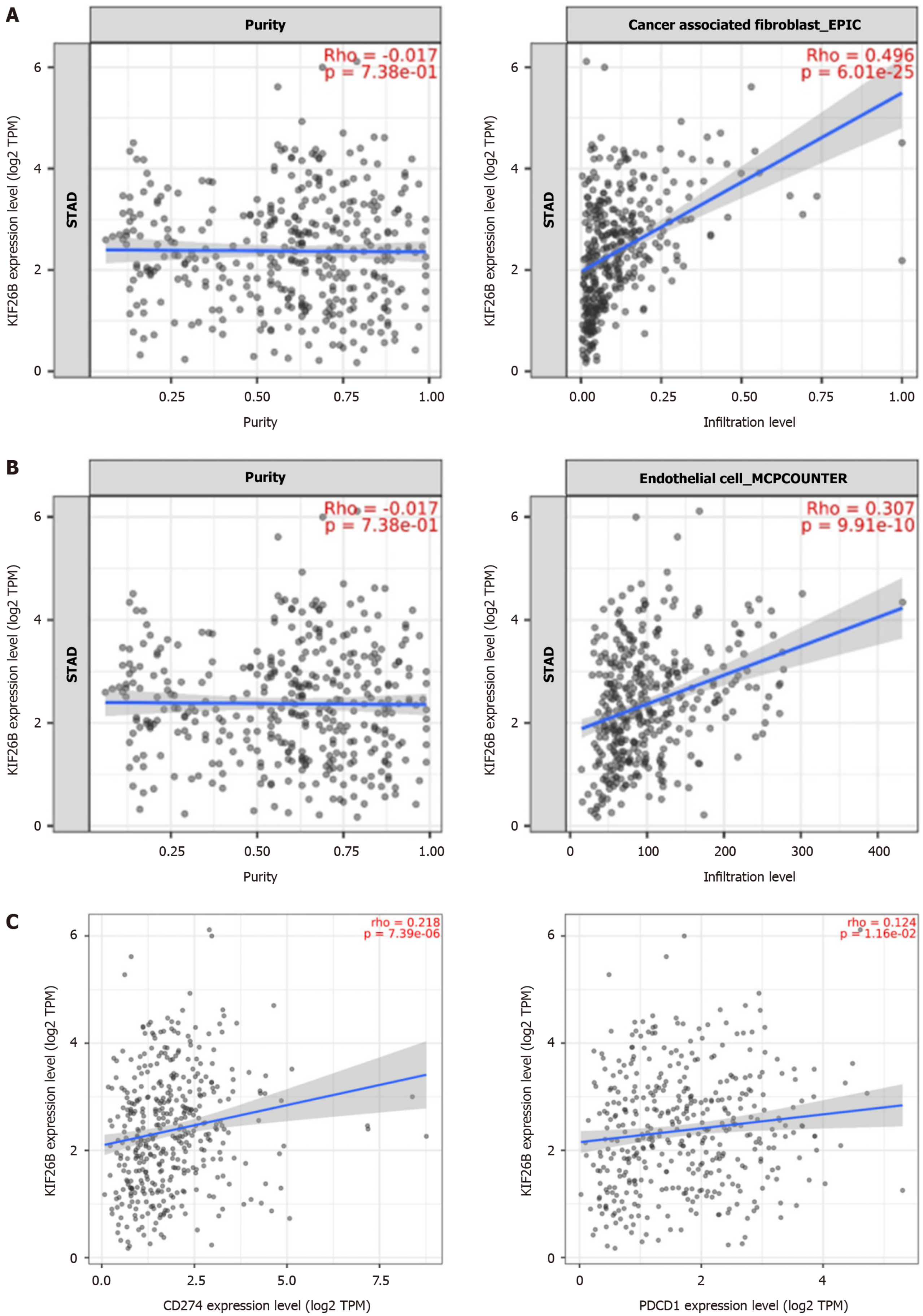
A
Purity
Rho = -0.017
p = 7.38e-01
STAD
KIF26B expression level (log2 TPM)
Purity
Cancer associated fibroblast_EPIC
Rho = 0.496
p = 6.01e-25
Infiltration level
B
Purity
Rho = -0.017
p = 7.38e-01
Endothelial cell_MCPCOUNTER
Rho = 0.307
p = 9.91e-10
Infiltration level
C
rho = 0.218
p = 7.39e-06
CD274 expression level (log2 TPM)
rho = 0.124
p = 1.16e-02
PDCD1 expression level (log2 TPM)

D

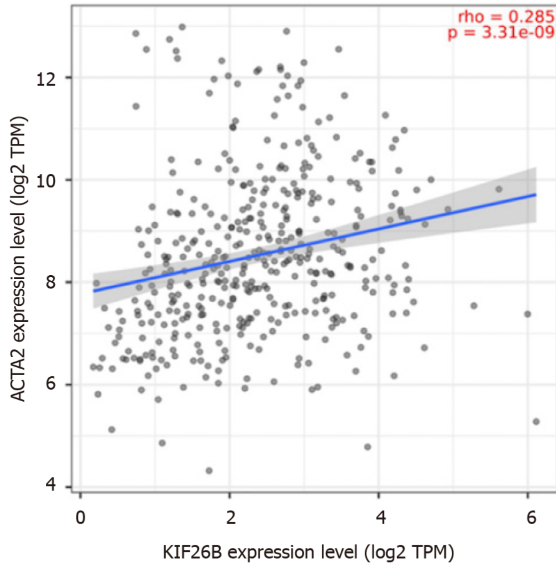

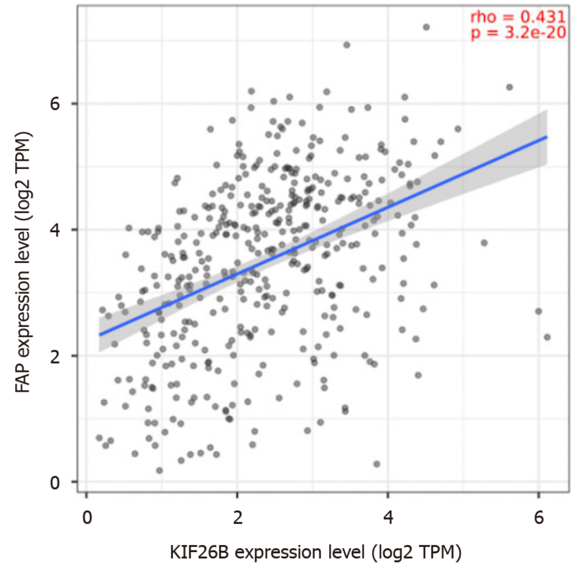

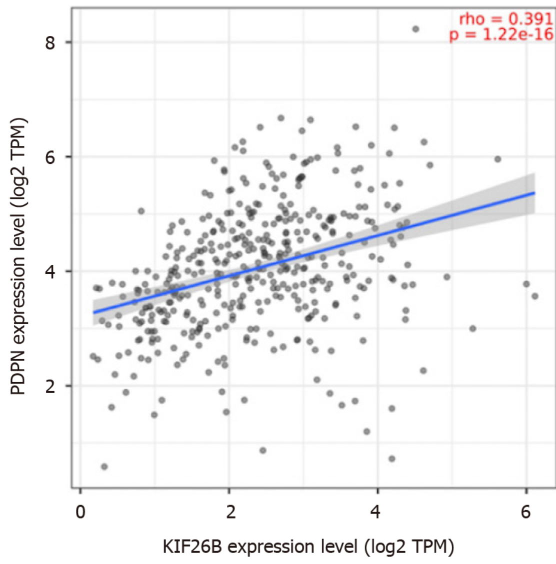

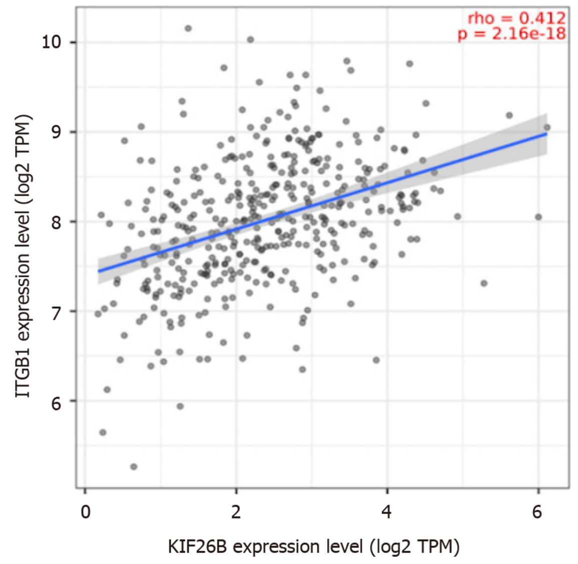

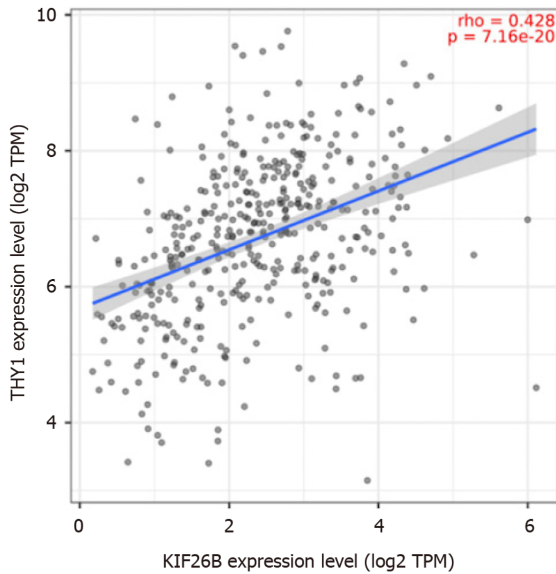

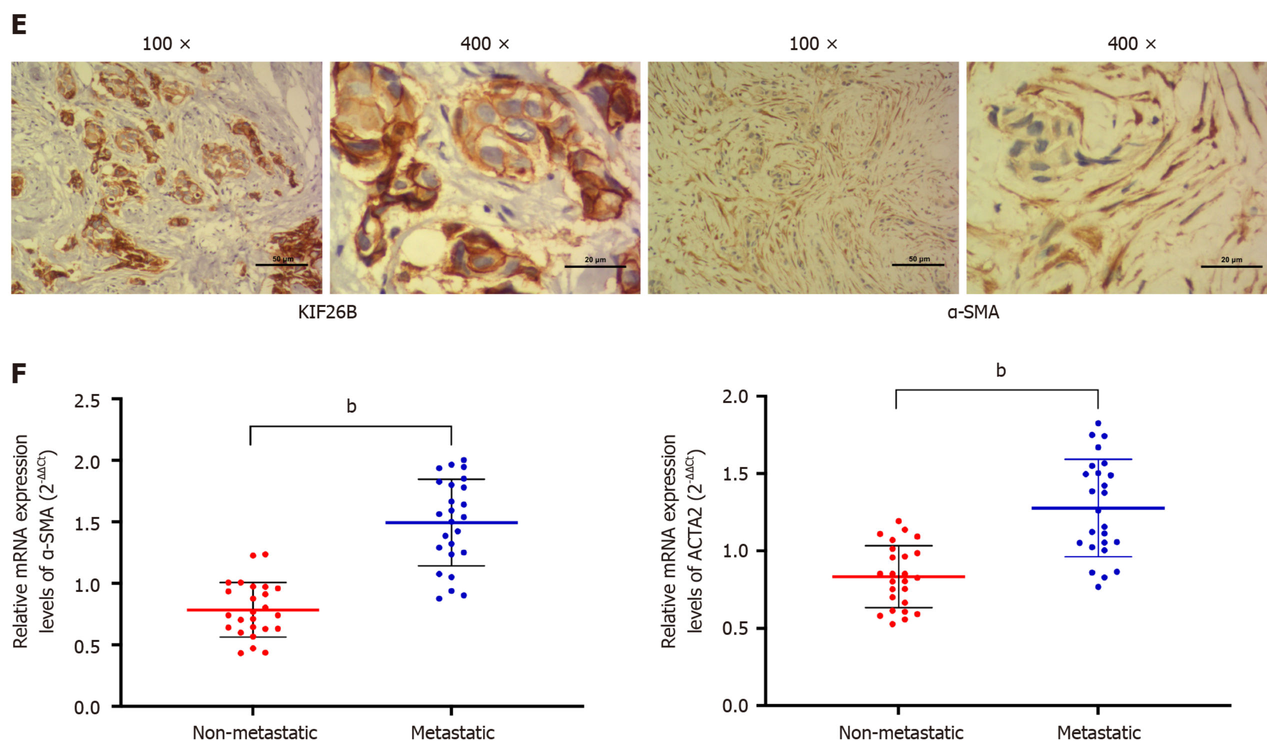

Figure 3 High expression of *KIF26B* may affect the activation or infiltration of gastric cancer related fibroblasts. A: Timer 2.0 analysis of the correlation between *KIF26B* expression and the degree of cancer-associated fibroblasts (CAFs) infiltration; B: Timer 2.0 analysis of the correlation between *KIF26B* expression and the degree of cancer endothelial cell infiltration; C: Timer 2.0 analysis of the correlation between *KIF26B* expression and *PD-1* (PDCD1), *PD-L1* (CD274) expression; D: Timer 2.0 analysis to verify the correlation between *KIF26B* and CAFs biomarkers (*ACTA2*, *FAP*, *ITGB1*, *PDPN*, and *THY1*); E: Immunohistochemical analysis of KIF26B and α-SMA in gastric cancer (GC) tissues (n = 3); F: The mRNA levels of CAFs Biomarker *α-SMA* and *ACTA2* in metastatic and non-metastatic GC tissues were detected by quantitative real-time polymerase chain reaction (n = 25). ^bP < 0.01.

with sh-NC group (Figure 5D). We counted macrophages using flow cytometry and found the number of M2 macrophages was a decreased in the sh-*KIF26B* group comparing with sh-NC group (Figure 5E). Data analysis found a significant positive correlation between *KIF26B* and chemokine *CXCL12* expression, and its corresponding receptor *CXCR4* (Figure 5F and G). *KIF26B* in GC cells may affect the M2 polarization of macrophage through CXCL12 secreted by CAFs.

KIF26B regulates M2 polarization of macrophages through fibroblast activation, regulating invasiveness, angiogenesis, and epithelial-mesenchymal transition processes of GC cells

We collected the supernatant of CAFs that transfected with sh-NC, sh-*KIF26B*, pcDNA-NC, and pcDNA-*KIF26B* as a conditioned medium to incubate GC cells (AGS and HGC-27 cells). Overexpression of *KIF26B* enhanced the migration and invasiveness of HGC-27 and AGS cells when compared with the negative control group, while knockdown of *KIF26B* could reduce the migration and invasiveness of AGS and HGC-27 cells (Figure 6A and B). Tube formation assay reported that the tube forming ability of cells was enhanced when *KIF26B* was overexpressed, and it was inhibited after *KIF26B* knockdown (Figure 6C). We detected epithelial-mesenchymal transition (EMT)-related protein expressions in HGC-27 and AGS cells, such as N-cadherin, E-cadherin, MMP2, and MMP9 (Figure 6D). While comparing with the control group, the sh-*KIF26B* group had lower N-cadherin, MMP2, and MMP9 protein expression levels, while the pcDNA-*KIF26B* group had higher N-cadherin, MMP2, and MMP9 protein expression levels, while the expression level of E-cadherin was opposite to other proteins (Figure 6D). M2 polarized macrophages' infiltration quantity in the pcDNA-*KIF26B* group was higher compared to the control group, while the infiltration quantity of M2 polarized macrophages in the sh-*KIF26B* group was lower (Figure 6E). Based on the above experimental results, it is revealed that *KIF26B* can regulate M2 polarization of macrophages through fibroblast activation, regulating invasiveness, angiogenesis, and EMT processes of GC cells.

DISCUSSION

GC is one of the most severe cancers globally[28,29]. Exploring GC progression mechanisms and developing new treatments have become necessary.

By analyzing the TCGA database, we discovered overexpression of *KIF26B* in most tumors. Highly expressed *KIF26B* was found in GC tissues and cells. Through survival analysis, we found that higher *KIF26B* expression was associated with poor GC prognosis. The clinical data analysis showed a high level of *KIF26B* significant association with invasion

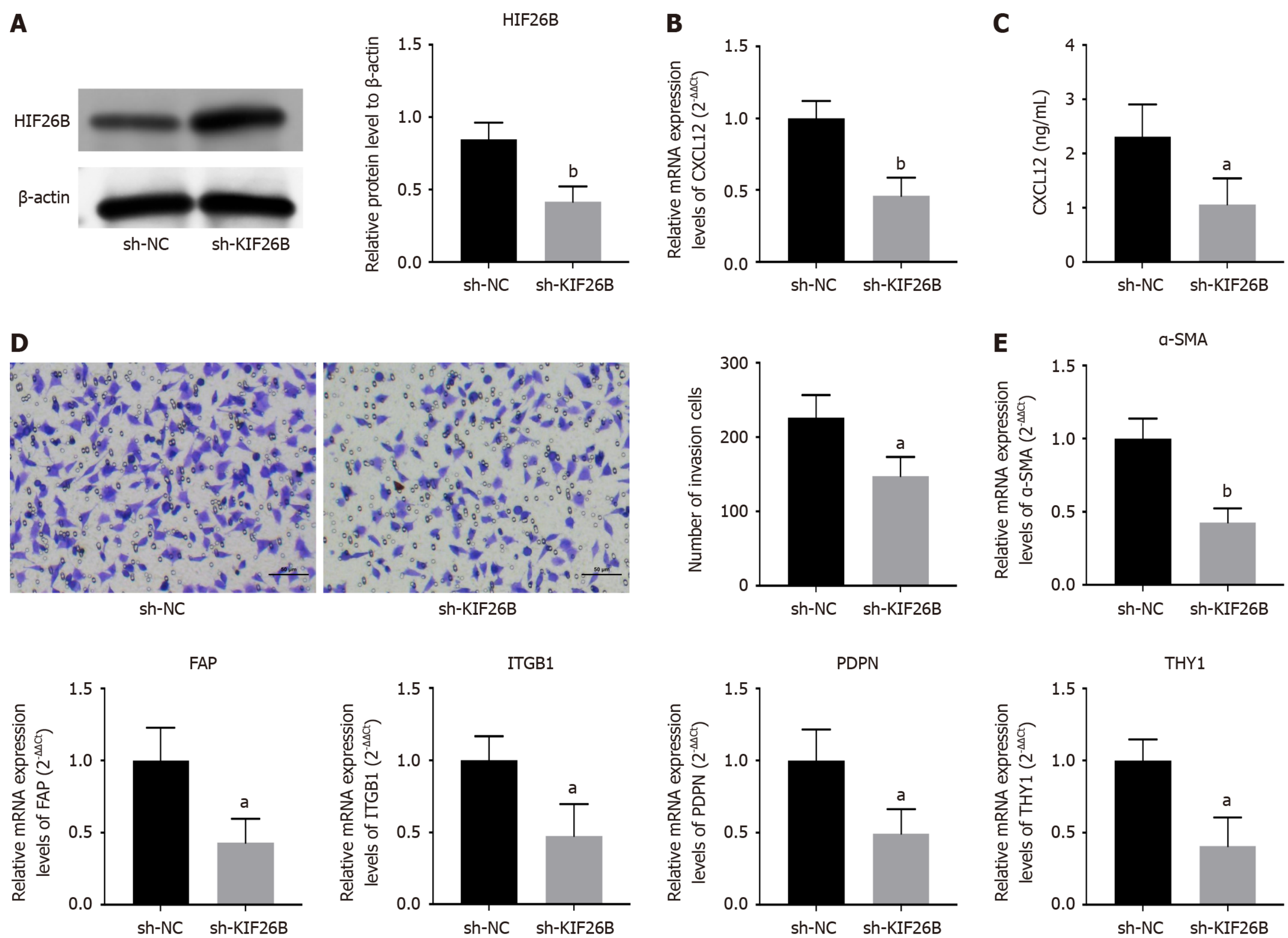

Figure 4 *KIF26B* affects the activation of fibroblasts to form the cancer-associated fibroblast phenotype. A: Detection of transfection efficiency of sh-*KIF26B* negative controls/sh-*KIF26B* in HGC-27 cells by Western blotting; B: ELISA assay for detecting the expression of chemokines (CXCL12) in HFF cells; C: Detection of mRNA expression levels of *CXCL12* in HFF cells by quantitative real-time polymerase chain reaction (qRT-PCR); D: Analyzing the invasive ability of HFF cells through Transwell assay; E: The expression levels of biomarkers (*α-SMA*, *FAP*, *ITGB1*, *PDPN* and *THY1*) for cancer-associated fibroblasts were detected by qRT-PCR. *n* = 3. $^aP < 0.05$, $^bP < 0.01$. sh-NC: sh-*KIF26B* negative controls.

depth, lymph node metastasis, and TNM stage of tumor. Like our results, Teng *et al*[30] reported that the level of *KIF26B* is significantly increased in breast cancer cells and tissues, and *KIF26B* level was positively related to the tumor size, TNM grading, and differentiation of breast cancer patients[30]. Data from Wang *et al*[31] suggest that *KIF26B* causes the occurrence of colorectal cancer (CC) and acts as a possible therapeutic target for CC[31]. Higher expression of *KIF26B* is observed in hepatocellular carcinoma tissues and cell lines[32]. Also, increased *KIF26B* expression is related to poor survival and differentiation and advanced TNM[32].

GC metastasis is the leading cause of death for patients[33], and the 5-year survival rate of patients in China with metastatic GC is less than 10%[34,35]. We found that knockdown of *KIF26B* decreased the occurrence, lung metastasis, and abdominal metastasis of GC. Previous research showed that *KIF26B* had an impact on the metastasis of breast cancer [30] and GC[13]. These are good supports for our results.

CAFs are essential to various tumors, such as GC[36,37]. CAFs aid in the invasion and metastasis of tumors during their occurrence and development[38]. The interaction mechanism between GC cells and CAFs is still unclear. A previous study found that knockdown of *KIF26B* inhibited the activation of renal fibroblasts[39]. We indicated that the high expression level of *KIF26B* promoted the activation and infiltration of CAFs through data analysis and experiments on GC tissues and cell lines. We found a positive relation between *KIF26B* expression and M2 macrophage activation. Cai *et al*[40] show that the fibroblast activating protein is associated with the invasion of M2 macrophages in gastrointestinal cancer[40]. Our subsequent experimental findings are similar to those of Cai *et al*[40] where *KIF26B* enhances crosstalk between tumor fibroblasts and macrophages, mediating the M2 polarization of macrophages. We found that *KIF26B* in GC cells might affect macrophage M2 polarization through CXCL12 secreted by CAFs.

The invasion[41], tube formation[42,43], and EMT process[44] of tumor cells are related to the cancer progression. Our research results indicated that *KIF26B* could regulate M2 polarization of macrophages through fibroblast activation, regulating tumor cell migration, invasion, angiogenesis, and EMT processes and completing the regulation of GC development and metastasis.

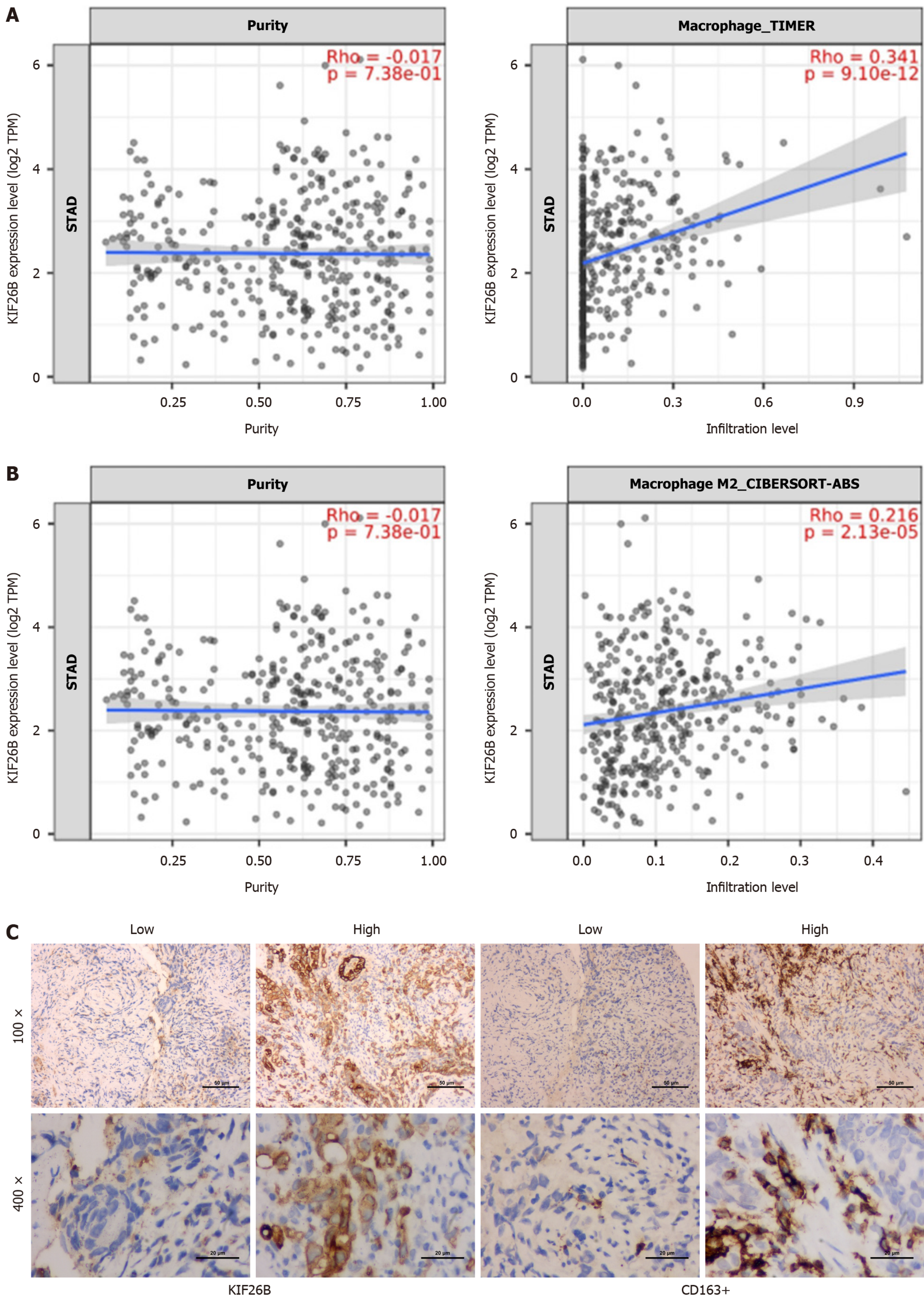
A
Purity
Rho = -0.017
p = 7.38e-01
STAD
KIF26B expression level (log2 TPM)
0.25
0.50
0.75
1.00
Purity
Macrophage_TIMER
Rho = 0.341
p = 9.10e-12
0.0
0.3
0.6
0.9
Infiltration level
B
Purity
Rho = -0.017
p = 7.38e-01
Macrophage M2_CIBERSORT-ABS
Rho = 0.216
p = 2.13e-05
0.0
0.1
0.2
0.3
0.4
Infiltration level
C
Low
High
Low
High
100 ×
400 ×
KIF26B
CD163+

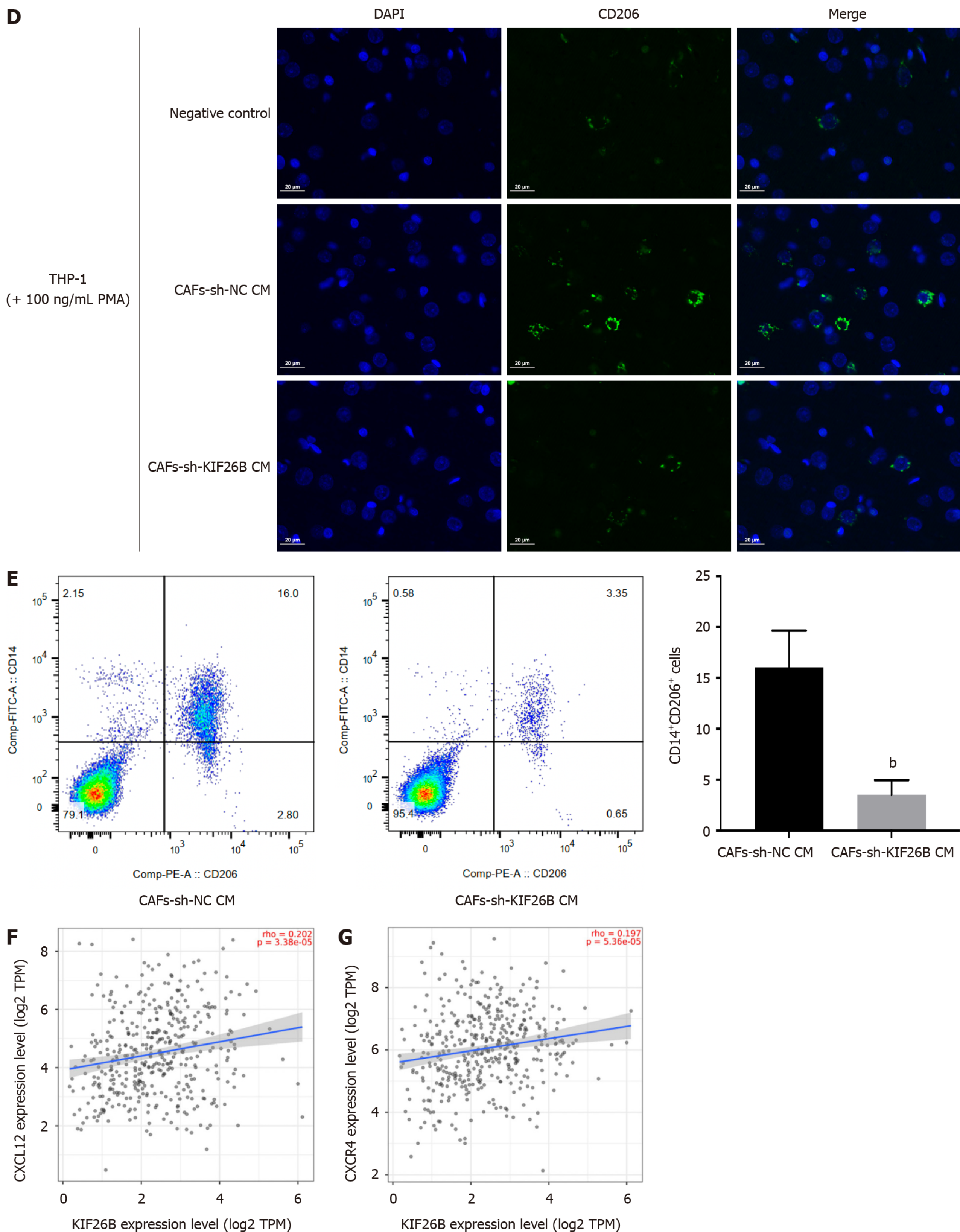

Figure 5 *KIF26B* enhances crosstalk between cancer-associated fibroblasts and macrophages, thereby mediating M2 polarization of macrophages. A: Timer 2.0 analysis of the correlation between *KIF26B* expression and macrophage activation; B: Timer 2.0 analysis of the correlation between *KIF26B* expression and M2 type macrophages; C: The correlation between the expression of KIF26B and the level of CD163+ (M2 macrophage marker) infiltration was analyzed by immunohistochemistry. *n* = 3; D: Immunofluorescence detection of CD206 signaling in THP-1 cells. The supernatant of cancer-associated fibroblasts that transfected with sh-KIF26B was used to incubate THP-1 cells. *n* = 3; E: Flow cytometry was used to detect the number of M2-polarized macrophages. *n* = 3; F: Analyzing the correlation between *KIF26B* expression and chemokine *CXCL12* expression through the Timer 2.0 database; G: Analyzing the correlation between *KIF26B* expression and *CXCR4* expression trough the Timer 2.0 database. $^{b}P < 0.01$. CAFs: Cancer-associated fibroblasts; sh-NC: sh-*KIF26B* negative controls.

A

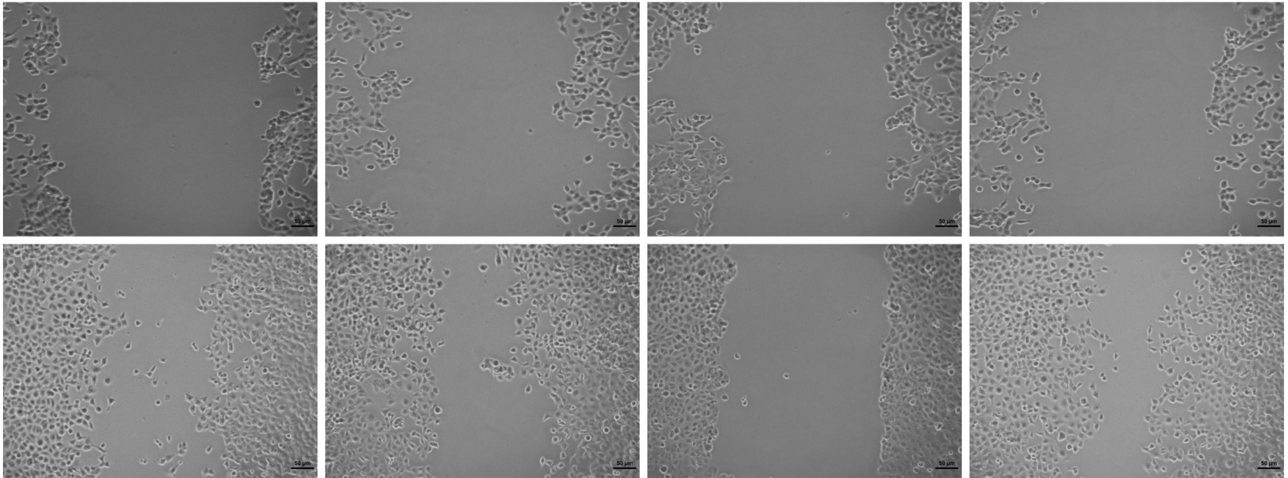

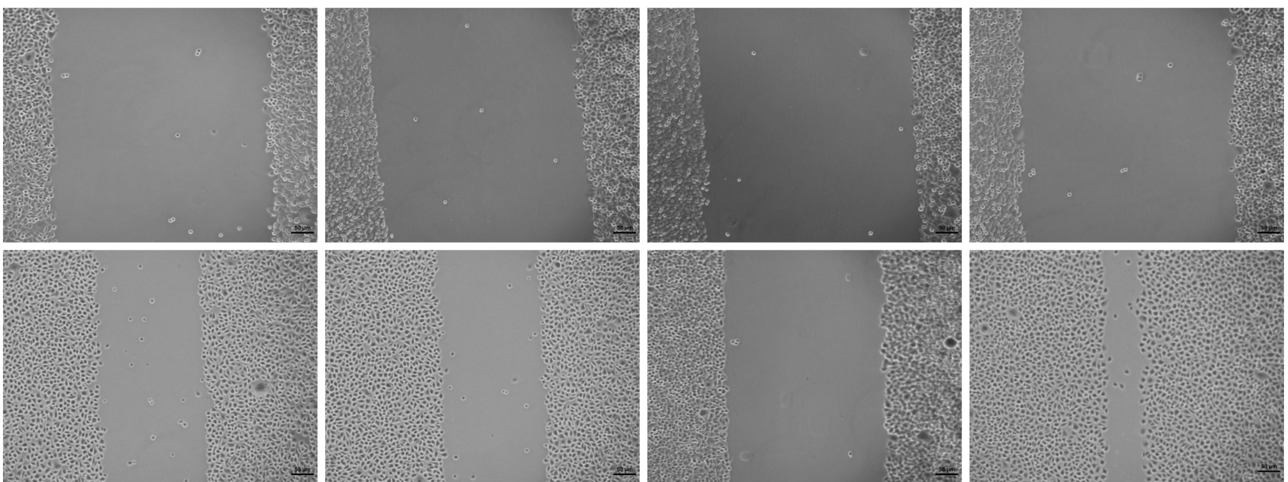

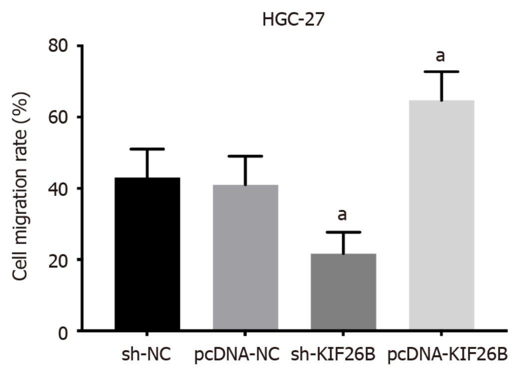

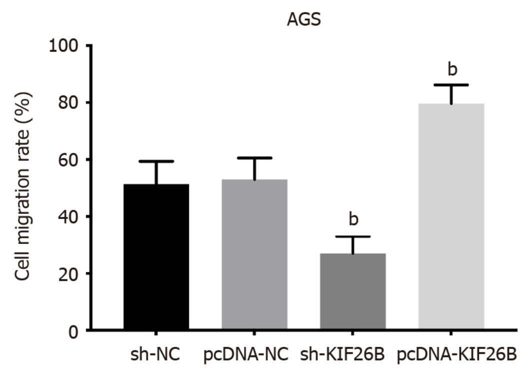

B

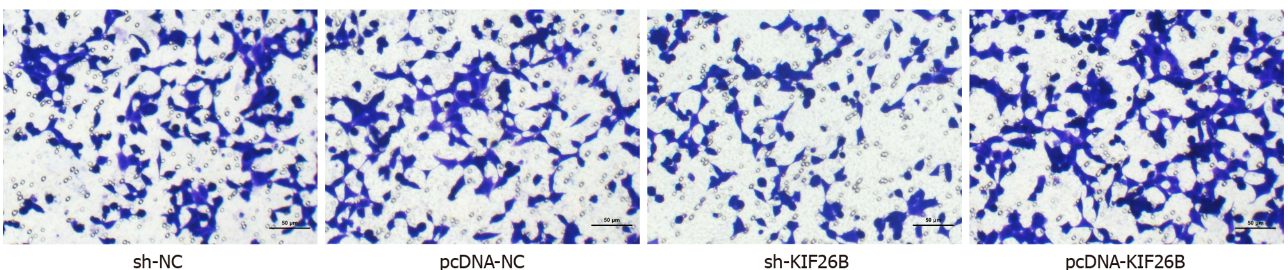

CAFs+AGS

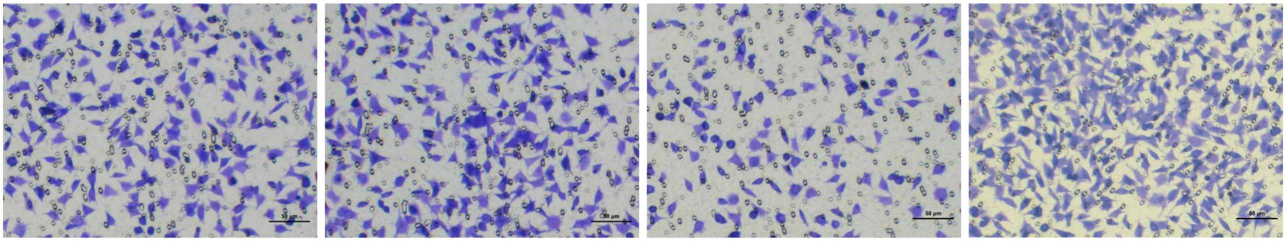

sh-NC pcDNA-NC sh-KIF26B pcDNA-KIF26B

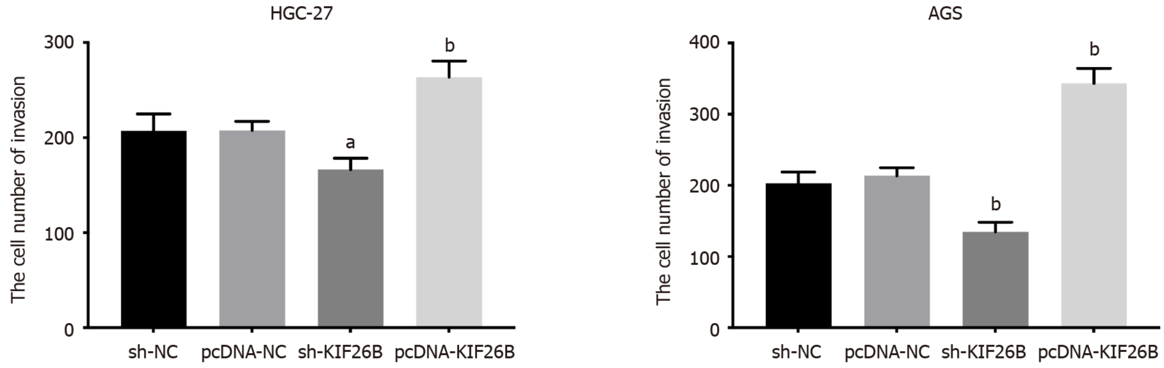

C

CAFs+HUVECS

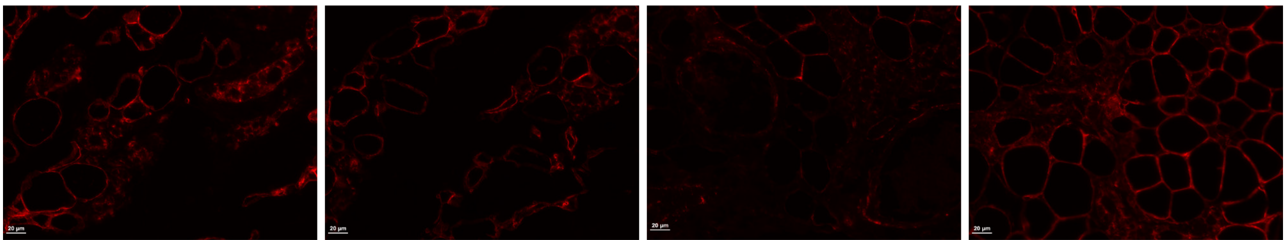

sh-NC pcDNA-NC sh-KIF26B pcDNA-KIF26B

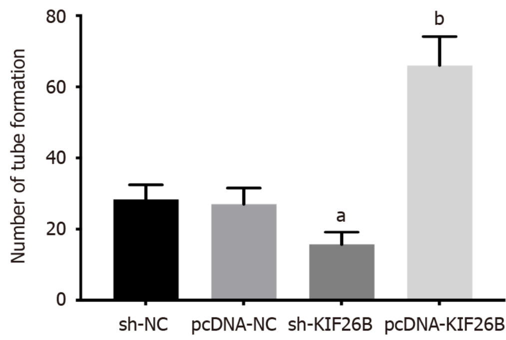

D

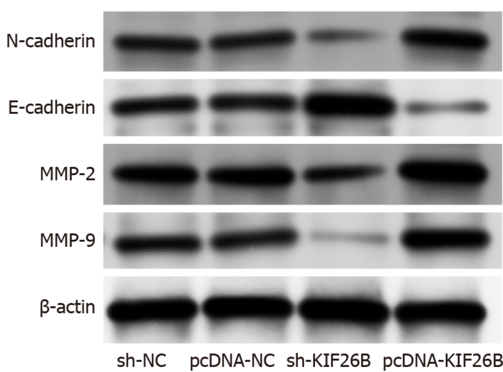

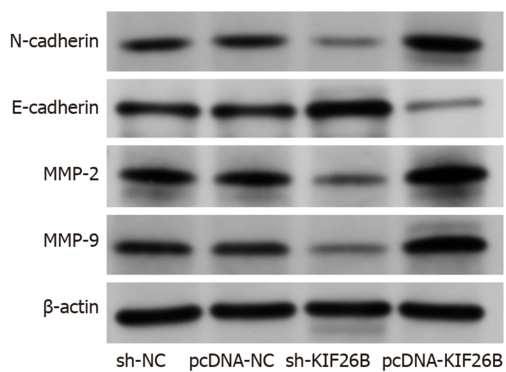

N-cadherin

Relative protein level to β-actin

sh-NC pcDNA-NC sh-KIF26B pcDNA-KIF26B

E-cadherin

Relative protein level to β-actin

sh-NC pcDNA-NC sh-KIF26B pcDNA-KIF26B

MMP2

Relative protein level to β-actin

sh-NC pcDNA-NC sh-KIF26B pcDNA-KIF26B

MMP9

Relative protein level to β-actin

sh-NC pcDNA-NC sh-KIF26B pcDNA-KIF26B

E

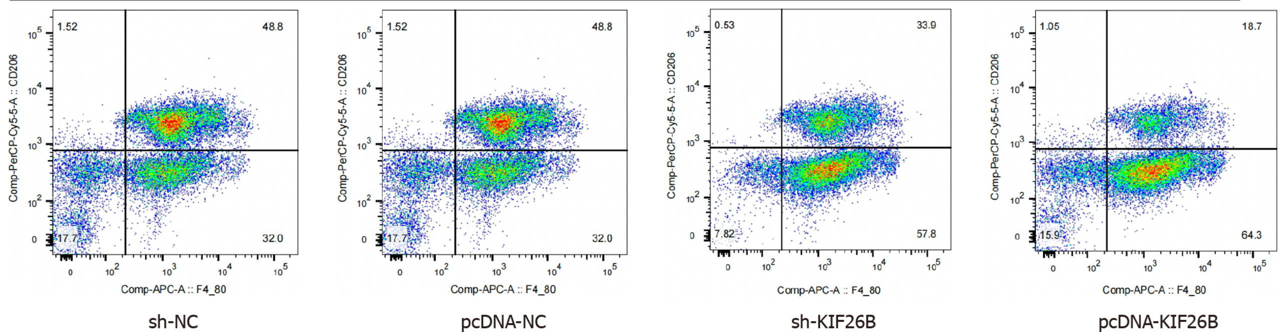

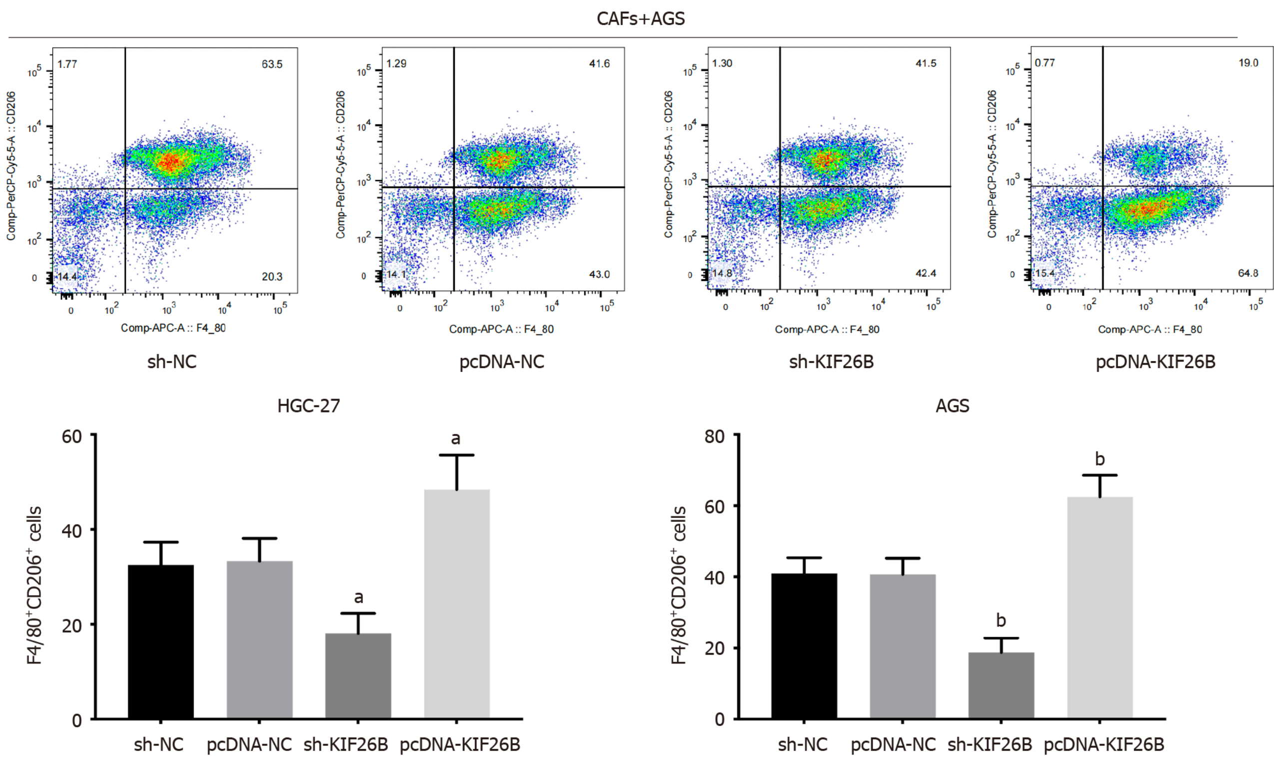

Figure 6 *KIF26B* regulates M2 polarization of macrophages through fibroblast activation, thereby regulating invasiveness, angiogenesis, and epithelial-mesenchymal transition processes of gastric cancer cells. A: The migration ability of HGC-27 and AGS cells was examined by wound healing assay; B: The invasiveness of HGC-27 and AGS cells were evaluated by Transwell assay; C: Endothelial cell tube formation assay was applied to detect the ability of HGC-27 and AGS cells to form tubes; D: Western blotting assay was used to detect the expression levels of epithelial-mesenchymal transition related proteins; E: The number of M2-polarized macrophage infiltration in HGC-27 and AGS cells was counted by flow cytometry. n = 3. $^aP < 0.05$, $^bP < 0.01$. CAFs: Cancer-associated fibroblasts; sh-NC: sh-*KIF26B* negative controls.

CONCLUSION

Although advances in basic and clinical studies have reduced the mortality rate of GC over the past decade, its prognosis remains poor due to incomplete diagnosis, high metastasis rate, and high chemotherapy resistance. We found that higher *KIF26B* expression could promote CAFs activation, mediating macrophage M2 polarization and affecting the occurrence, lung metastasis, and abdominal metastasis of GC. This study provides useful insights for exploring new mechanisms of GC and delaying its progression.

FOOTNOTES

Author contributions: Huang LM contributed to conceptualization, writing original draft; Huang LM and Zhang MJ contributed to data curation, formal analysis, writing - review and editing.

Institutional review board statement: This study was approved by the Medical Ethics Committee of The 901st Hospital of PLA (No. 202311006). The written consent from each participant has been acquired.

Institutional animal care and use committee statement: All animal experiments were approved by the Animal Ethics Committee of Beijing Viewsolid Biotechnology Co. LTD (No. VS2126A00168).

Conflict-of-interest statement: All the authors report no relevant conflicts of interest for this article.

Data sharing statement: The data that support the findings of this study are available from the corresponding author at zhangmingjin2001@163.com.

ARRIVE guidelines statement: The authors have read the ARRIVE Guidelines, and the manuscript was prepared and revised according to the ARRIVE Guidelines.

Open-Access: This article is an open-access article that was selected by an in-house editor and fully peer-reviewed by external reviewers. It is distributed in accordance with the Creative Commons Attribution NonCommercial (CC BY-NC 4.0) license, which permits others to distribute, remix, adapt, build upon this work non-commercially, and license their derivative works on different terms, provided the

original work is properly cited and the use is non-commercial. See: https://creativecommons.org/Licenses/by-nc/4.0/

Country of origin: China

ORCID number: Ming-Jin Zhang 0009-0003-7026-7691.

S-Editor: Li L
L-Editor: A
P-Editor: Yuan YY

REFERENCES

1 **Miki H**, Setou M, Kaneshiro K, Hirokawa N. All kinesin superfamily protein, KIF, genes in mouse and human. *Proc Natl Acad Sci U S A* 2001; **98**: 7004-7011 [PMID: 11416179 DOI: 10.1073/pnas.111145398]

2 **Hirokawa N**, Noda Y. Intracellular transport and kinesin superfamily proteins, KIFs: structure, function, and dynamics. *Physiol Rev* 2008; **88**: 1089-1118 [PMID: 18626067 DOI: 10.1152/physrev.00023.2007]

3 **Hirokawa N**, Noda Y, Tanaka Y, Niwa S. Kinesin superfamily motor proteins and intracellular transport. *Nat Rev Mol Cell Biol* 2009; **10**: 682-696 [PMID: 19773780 DOI: 10.1038/nrm2774]

4 **Li X**, Tai Y, Liu S, Gao Y, Zhang K, Yin J, Zhang H, Wang X, Li X, Zhang D. Bioinformatics analysis: relationship between adrenocortical carcinoma and KIFs. *Biotechnol Genet Eng Rev* 2022; 1-11 [PMID: 36572958 DOI: 10.1080/02648725.2022.2160560]

5 **Li TF**, Zeng HJ, Shan Z, Ye RY, Cheang TY, Zhang YJ, Lu SH, Zhang Q, Shao N, Lin Y. Overexpression of kinesin superfamily members as prognostic biomarkers of breast cancer. *Cancer Cell Int* 2020; **20**: 123 [PMID: 32322170 DOI: 10.1186/s12935-020-01191-1]

6 **Lucanus AJ**, Yip GW. Kinesin superfamily: roles in breast cancer, patient prognosis and therapeutics. *Oncogene* 2018; **37**: 833-838 [PMID: 29059174 DOI: 10.1038/onc.2017.406]

7 **Wu Z**, Zhang H, Sun Z, Wang C, Chen Y, Luo P, Yan W. Knockdown of Kinesin Family 15 Inhibits Osteosarcoma through Suppressing Cell Proliferation and Promoting Cell Apoptosis. *Chemotherapy* 2019; **64**: 187-196 [PMID: 32074608 DOI: 10.1159/000505014]

8 **Zhou J**, Chen WR, Yang LC, Wang J, Sun JY, Zhang WW, He ZY, Wu SG. KIF11 Functions as an Oncogene and Is Associated with Poor Outcomes from Breast Cancer. *Cancer Res Treat* 2019; **51**: 1207-1221 [PMID: 30590004 DOI: 10.4143/crt.2018.460]

9 **Li ZY**, Wang ZX, Li CC. Kinesin family member 20B regulates tongue cancer progression by promoting cell proliferation. *Mol Med Rep* 2019; **19**: 2202-2210 [PMID: 30664160 DOI: 10.3892/mmr.2019.9851]

10 **Sheng J**, Xue X, Jiang K. Knockdown of Kinase Family 15 Inhibits Cancer Cell Proliferation In vitro and its Clinical Relevance in Triple-Negative Breast Cancer. *Curr Mol Med* 2019; **19**: 147-155 [PMID: 30854965 DOI: 10.2174/1566524019666190308122108]

11 **Ding L**, Li B, Yu X, Li Z, Li X, Dang S, Lv Q, Wei J, Sun H, Chen H, Liu M, Li G. KIF15 facilitates gastric cancer *via* enhancing proliferation, inhibiting apoptosis, and predict poor prognosis. *Cancer Cell Int* 2020; **20**: 125 [PMID: 32322172 DOI: 10.1186/s12935-020-01199-7]

12 **Zhao P**, Lan F, Zhang H, Zeng G, Liu D. Down-regulation of KIF2A inhibits gastric cancer cell invasion *via* suppressing MT1-MMP. *Clin Exp Pharmacol Physiol* 2018; **45**: 1010-1018 [PMID: 29781531 DOI: 10.1111/1440-1681.12974]

13 **Zhang H**, Ma RR, Wang XJ, Su ZX, Chen X, Shi DB, Guo XY, Liu HT, Gao P. KIF26B, a novel oncogene, promotes proliferation and metastasis by activating the VEGF pathway in gastric cancer. *Oncogene* 2017; **36**: 5609-5619 [PMID: 28581513 DOI: 10.1038/onc.2017.163]

14 **Xiao Y**, Yu D. Tumor microenvironment as a therapeutic target in cancer. *Pharmacol Ther* 2021; **221**: 107753 [PMID: 33259885 DOI: 10.1016/j.pharmthera.2020.107753]

15 **Hinshaw DC**, Shevde LA. The Tumor Microenvironment Innately Modulates Cancer Progression. *Cancer Res* 2019; **79**: 4557-4566 [PMID: 31350295 DOI: 10.1158/0008-5472.CAN-18-3962]

16 **Deepak KGK**, Vempati R, Nagaraju GP, Dasari VR, S N, Rao DN, Malla RR. Tumor microenvironment: Challenges and opportunities in targeting metastasis of triple negative breast cancer. *Pharmacol Res* 2020; **153**: 104683 [PMID: 32050092 DOI: 10.1016/j.phrs.2020.104683]

17 **Bader JE**, Voss K, Rathmell JC. Targeting Metabolism to Improve the Tumor Microenvironment for Cancer Immunotherapy. *Mol Cell* 2020; **78**: 1019-1033 [PMID: 32559423 DOI: 10.1016/j.molcel.2020.05.034]

18 **Pitt JM**, Marabelle A, Eggermont A, Soria JC, Kroemer G, Zitvogel L. Targeting the tumor microenvironment: removing obstruction to anticancer immune responses and immunotherapy. *Ann Oncol* 2016; **27**: 1482-1492 [PMID: 27069014 DOI: 10.1093/annonc/mdw168]

19 **Kalluri R**, Zeisberg M. Fibroblasts in cancer. *Nat Rev Cancer* 2006; **6**: 392-401 [PMID: 16572188 DOI: 10.1038/nrc1877]

20 **Sun F**, Lian Y, Wang J, Hu L, Luo J, Yu J. KIF26B in the Prognosis and Immune Biomarking of Various Cancers: A Pan-Cancer Study. *J Oncol* 2022; **2022**: 4829697 [PMID: 35359341 DOI: 10.1155/2022/4829697]

21 **Lewis CE**, Pollard JW. Distinct role of macrophages in different tumor microenvironments. *Cancer Res* 2006; **66**: 605-612 [PMID: 16423985 DOI: 10.1158/0008-5472.CAN-05-4005]

22 **Ma J**, Liu L, Che G, Yu N, Dai F, You Z. The M1 form of tumor-associated macrophages in non-small cell lung cancer is positively associated with survival time. *BMC Cancer* 2010; **10**: 112 [PMID: 20338029 DOI: 10.1186/1471-2407-10-112]

23 **Ong SM**, Tan YC, Beretta O, Jiang D, Yeap WH, Tai JJ, Wong WC, Yang H, Schwarz H, Lim KH, Koh PK, Ling KL, Wong SC. Macrophages in human colorectal cancer are pro-inflammatory and prime T cells towards an anti-tumour type-1 inflammatory response. *Eur J Immunol* 2012; **42**: 89-100 [PMID: 22009685 DOI: 10.1002/eji.201141825]

24 **Rhee I**. Diverse macrophages polarization in tumor microenvironment. *Arch Pharm Res* 2016; **39**: 1588-1596 [PMID: 27562774 DOI: 10.1007/s12272-016-0820-y]

25 **Zhang M**, He Y, Sun X, Li Q, Wang W, Zhao A, Di W. A high M1/M2 ratio of tumor-associated macrophages is associated with extended survival in ovarian cancer patients. *J Ovarian Res* 2014; **7**: 19 [PMID: 24507759 DOI: 10.1186/1757-2215-7-19]

26 **Wei C**, Yang C, Wang S, Shi D, Zhang C, Lin X, Liu Q, Dou R, Xiong B. Crosstalk between cancer cells and tumor associated macrophages is required for mesenchymal circulating tumor cell-mediated colorectal cancer metastasis. *Mol Cancer* 2019; **18**: 64 [PMID: 30927925 DOI: 10.1186/s12943-019-0976-4]

27 **Li X**, Sun Z, Peng G, Xiao Y, Guo J, Wu B, Li X, Zhou W, Li J, Li Z, Bai C, Zhao L, Han Q, Zhao RC, Wang X. Single-cell RNA sequencing reveals a pro-invasive cancer-associated fibroblast subgroup associated with poor clinical outcomes in patients with gastric cancer. *Theranostics* 2022; **12**: 620-638 [PMID: 34976204 DOI: 10.7150/thno.60540]

28 **Deng H**, Gao J, Cao B, Qiu Z, Li T, Zhao R, Li H, Wei B. LncRNA CCAT2 promotes malignant progression of metastatic gastric cancer through regulating CD44 alternative splicing. *Cell Oncol (Dordr)* 2023; **46**: 1675-1690 [PMID: 37354353 DOI: 10.1007/s13402-023-00835-4]

29 **Chen G**, Luo D, Qi X, Li D, Zheng J, Luo Y, Zhang C, Ren Q, Lu Y, Chan YT, Chen B, Wu J, Wang N, Feng Y. Characterization of cuproptosis in gastric cancer and relationship with clinical and drug reactions. *Front Cell Dev Biol* 2023; **11**: 1172895 [PMID: 37351275 DOI: 10.3389/fcell.2023.1172895]

30 **Teng Y**, Guo B, Mu X, Liu S. KIF26B promotes cell proliferation and migration through the FGF2/ERK signaling pathway in breast cancer. *Biomed Pharmacother* 2018; **108**: 766-773 [PMID: 30248545 DOI: 10.1016/j.biopha.2018.09.036]

31 **Wang J**, Cui F, Wang X, Xue Y, Chen J, Yu Y, Lu H, Zhang M, Tang H, Peng Z. Elevated kinesin family member 26B is a prognostic biomarker and a potential therapeutic target for colorectal cancer. *J Exp Clin Cancer Res* 2015; **34**: 13 [PMID: 25652119 DOI: 10.1186/s13046-015-0129-6]

32 **Li H**, Shen S, Chen X, Ren Z, Li Z, Yu Z. miR-450b-5p loss mediated KIF26B activation promoted hepatocellular carcinoma progression by activating PI3K/AKT pathway. *Cancer Cell Int* 2019; **19**: 205 [PMID: 31388332 DOI: 10.1186/s12935-019-0923-x]

33 **Yu B**, Zhu N, Fan Z, Li J, Kang Y, Liu B. miR-29c inhibits metastasis of gastric cancer cells by targeting VEGFA. *J Cancer* 2022; **13**: 3566-3574 [PMID: 36484007 DOI: 10.7150/jca.77727]

34 **Chen W**, Sun K, Zheng R, Zeng H, Zhang S, Xia C, Yang Z, Li H, Zou X, He J. Cancer incidence and mortality in China, 2014. *Chin J Cancer Res* 2018; **30**: 1-12 [PMID: 29545714 DOI: 10.21147/j.issn.1000-9604.2018.01.01]

35 **Chen W**, Zheng R, Baade PD, Zhang S, Zeng H, Bray F, Jemal A, Yu XQ, He J. Cancer statistics in China, 2015. *CA Cancer J Clin* 2016; **66**: 115-132 [PMID: 26808342 DOI: 10.3322/caac.21338]

36 **Zhao X**, He Y, Gao J, Fan L, Li Z, Yang G, Chen H. Caveolin-1 expression level in cancer associated fibroblasts predicts outcome in gastric cancer. *PLoS One* 2013; **8**: e59102 [PMID: 23527097 DOI: 10.1371/journal.pone.0059102]

37 **Özdemir BC**, Pentcheva-Hoang T, Carstens JL, Zheng X, Wu CC, Simpson TR, Laklai H, Sugimoto H, Kahlert C, Novitskiy SV, De Jesus-Acosta A, Sharma P, Heidari P, Mahmood U, Chin L, Moses HL, Weaver VM, Maitra A, Allison JP, LeBleu VS, Kalluri R. Depletion of carcinoma-associated fibroblasts and fibrosis induces immunosuppression and accelerates pancreas cancer with reduced survival. *Cancer Cell* 2014; **25**: 719-734 [PMID: 24856586 DOI: 10.1016/j.ccr.2014.04.005]

38 **Chung HW**, Lim JB. Role of the tumor microenvironment in the pathogenesis of gastric carcinoma. *World J Gastroenterol* 2014; **20**: 1667-1680 [PMID: 24587646 DOI: 10.3748/wjg.v20.i7.1667]

39 **Yamamura Y**, Iwata Y, Furuichi K, Kato T, Yamamoto N, Horikoshi K, Ogura H, Sato K, Oshima M, Nakagawa S, Miyagawa T, Kitajima S, Toyama T, Hara A, Sakai N, Shimizu M, Horike S, Daikoku T, Nishinakamura R, Wada T. Kif26b contributes to the progression of interstitial fibrosis *via* migration and myofibroblast differentiation in renal fibroblast. *FASEB J* 2022; **36**: e22606 [PMID: 36250931 DOI: 10.1096/fj.202200355R]

40 **Cai J**, Yang D, Sun H, Xiao L, Han F, Zhang M, Zhou L, Jiang M, Jiang Q, Li Y, Nie H. A multifactorial analysis of FAP to regulate gastrointestinal cancers progression. *Front Immunol* 2023; **14**: 1183440 [PMID: 37325617 DOI: 10.3389/fimmu.2023.1183440]

41 **Li S**, Cong X, Gao H, Lan X, Li Z, Wang W, Song S, Wang Y, Li C, Zhang H, Zhao Y, Xue Y. Tumor-associated neutrophils induce EMT by IL-17a to promote migration and invasion in gastric cancer cells. *J Exp Clin Cancer Res* 2019; **38**: 6 [PMID: 30616627 DOI: 10.1186/s13046-018-1003-0]

42 **Gianni-Barrera R**, Di Maggio N, Melly L, Burger MG, Mujagic E, Gürke L, Schaefer DJ, Banfi A. Therapeutic vascularization in regenerative medicine. *Stem Cells Transl Med* 2020; **9**: 433-444 [PMID: 31922362 DOI: 10.1002/sctm.19-0319]

43 **Yang Y**, Cao Y. The impact of VEGF on cancer metastasis and systemic disease. *Semin Cancer Biol* 2022; **86**: 251-261 [PMID: 35307547 DOI: 10.1016/j.semcancer.2022.03.011]

44 **Tian S**, Peng P, Li J, Deng H, Zhan N, Zeng Z, Dong W. SERPINH1 regulates EMT and gastric cancer metastasis *via* the Wnt/β-catenin signaling pathway. *Aging (Albany NY)* 2020; **12**: 3574-3593 [PMID: 32091407 DOI: 10.18632/aging.102831]

Published by **Baishideng Publishing Group Inc**
7041 Koll Center Parkway, Suite 160, Pleasanton, CA 94566, USA
Telephone: +1-925-3991568
E-mail: office@baishideng.com
Help Desk: https://www.f6publishing.com/helpdesk
https://www.wjgnet.com

© 2024 Baishideng Publishing Group Inc. All rights reserved.